LETTERS

Modulation of intracortical synaptic potentials by presynaptic somatic membrane potential

Yousheng Shu[1], Andrea Hasenstaub[1], Alvaro Duque[1], Yuguo Yu[1] & David A. McCormick[1]

Traditionally, neuronal operations in the cerebral cortex have been viewed as occurring through the interaction of synaptic potentials in the dendrite and soma, followed by the initiation of an action potential, typically in the axon[1,2]. Propagation of this action potential to the synaptic terminals is widely believed to be the only form of rapid communication of information between the soma and axonal synapses, and hence to postsynaptic neurons. Here we show that the voltage fluctuations associated with dendrosomatic synaptic activity propagate significant distances along the axon, and that modest changes in the somatic membrane potential of the presynaptic neuron modulate the amplitude and duration of axonal action potentials and, through a Ca^{2+}-dependent mechanism, the average amplitude of the postsynaptic potential evoked by these spikes. These results indicate that synaptic activity in the dendrite and soma controls not only the pattern of action potentials generated, but also the amplitude of the synaptic potentials that these action potentials initiate in local cortical circuits, resulting in synaptic transmission that is a mixture of triggered and graded (analogue) signals.

To examine the properties of monosynaptic excitatory connections within the cortex, we obtained whole-cell recordings from nearby (within 60 μm) and synaptically connected pairs of layer 5 pyramidal cells in ferret prefrontal cortical slices (Fig. 1, $n = 28$ paired recordings; Supplementary Fig. 1). As expected, activation of an action potential in the presynaptic neuron with a short (1 ms) depolarizing current pulse resulted in an excitatory postsynaptic potential (EPSP; Fig. 1b). However, we found that steady depolarization of the soma of the presynaptic neuron by approximately 10–15 mV from the resting membrane potential (average −62 mV) to near the firing threshold (average −48 mV) resulted in a substantial and statistically significant increase in the average EPSP amplitude evoked in the postsynaptic cell (18/28 synaptic connections in 28 unique paired recordings; Fig. 1b, e), even though this depolarization had no significant effect on the resting membrane potential of the postsynaptic cell. The median significant enhancement was 29% (ranging from 12 to 69%, with one outlier at 194%; Fig. 1e) and was reversible (Fig. 1b).

We observed the enhancing effect of presynaptic somatic membrane potential even if the hyperpolarized and depolarized periods were 10–20 s in duration each and intermixed (Fig. 1c, d; $n = 19/37$ synaptic connections in 33 pairs tested). We examined the kinetics of the enhancing effect of presynaptic somatic depolarization on EPSP amplitude in paired recordings and found that the enhancement seemed to have both rapid (<1 s) and slower (>1 s) components (Fig. 1f). The disfacilitation upon subsequent hyperpolarization exhibited a slow decrease that could be well fitted ($r^2 = 0.92$) by an exponential function with $\tau = 4.3$ s ($n = 10$, Fig. 1f; see also Supplementary Fig. 2).

We examined a range of voltages and found that the average amplitude of the evoked EPSP steadily increases as a nearly linear function of the somatic membrane potential of the presynaptic cell, ranging from 26 to 258% over the 15–24 mV range tested (Fig. 2a, $n = 5$). The average slope of the linear fits was 31.2 ± 44.8% enhancement of EPSP amplitude per 10 mV of presynaptic depolarization. EPSPs of all amplitudes showed facilitation (Fig. 2a), but there was no significant relationship between EPSP amplitude and per cent facilitation ($r = -0.22$, $P = 0.26$; data not shown). Examination of the distribution of amplitudes of single evoked EPSPs revealed that presynaptic-depolarization-induced facilitation resulted in a rightward shift of the EPSP amplitude histogram (Fig. 2b, c; $n = 15$) and cumulative EPSP amplitude distribution (Supplementary Fig. 3).

One possible mechanism for this facilitatory effect is that depolarization of the somata of pyramidal neurons results in depolarization of their nearby synaptic terminals. Depolarization is known to strongly increase transmitter release at central synapses (with an increase of 10% per mV in one study[3]), perhaps through small increases in intracellular calcium ($[Ca^{2+}]_i$). To test this possibility, we recorded from neurons using pipettes that contained the calcium chelators BAPTA (25 μM) and either 10 mM EGTA ($n = 16$) or 1 mM EGTA ($n = 11$). The concentrations of EGTA and BAPTA at the relevant sites of synaptic transmission between the two recorded neurons are not known and may be substantially lower. In cells recorded with 10 mM EGTA, somatic-depolarization-induced enhancement of EPSPs was observed in only 1/16 pairs ($P < 0.01$ by χ^2 test, compared to BAPTA alone), whereas facilitation was observed in 3/11 pairs recorded with 1 mM EGTA ($P = 0.08$).

Facilitation of action-potential-triggered PSPs by somatic depolarization has been observed in several invertebrate preparations and seems to occur through an increase in the probability of transmitter release, either by depolarization of synapses that are electrotonically close to the soma, or by broadening of the action potential[4–7]. To investigate which of these may account for our facilitation effect, we obtained simultaneous GΩ seal, whole-cell recordings from the somata and axons of layer 5 pyramidal cells (for example, see Fig. 4c; $n = 76$). Axonal whole-cell recordings were possible because cortical axons form spherical 4–6-μm diameter 'bleb'-like structures at the surface of the slice in response to the slicing procedure. Although this structure is certainly abnormal in some regards, whole-cell recordings from the axon bleb will reflect the action potential properties of the main axon, owing to the electrotonic compactness of these structures. Depolarization of the soma of layer 5 pyramidal neurons significantly increased the duration, decreased the amplitude and increased the integrated area (mV × ms) of action potentials recorded in the axon, even up to 300 μm from the soma (Fig. 3), especially near the firing threshold. Changes in action potential duration with depolarization of the soma occurred very rapidly in the cell body, being complete within 100 ms (Fig. 3e, $n = 9$; see also Supplementary Fig. 2). In contrast, changes in action potential duration in the distal (90–400 μm) axon occurred more

[1]Department of Neurobiology, Kavli Institute for Neuroscience, Yale University School of Medicine, 333 Cedar Street, New Haven, Connecticut 06510, USA.

© 2006 Nature Publishing Group

slowly. Action potential broadening had a time constant of 2.3 s with depolarization of the soma, whereas hyperpolarization of the soma shortened axonal action potentials, also with a slow time course ($\tau = 1.5$ s, $n = 9$; Fig. 3f), even though changes in somatic membrane potential were rapidly (within 25 ms) reflected in the axonal membrane potential. Changes in the duration of axonal action potentials occurred through changes in the falling phase, and are suggestive of the slow inactivation and removal of inactivation of K^+ currents important for axonal action potential repolarization[8].

It has previously been shown in cultured hippocampal pyramidal neurons that the A-current can gate axon conduction, resulting in apparent axon conduction failures from hyperpolarized membrane potentials[9]. However, we failed to observe any failures of orthodromic axon conduction along the main axon—even several hundred micrometres from the soma—at any of the membrane potentials tested (−80 to −50 mV, $n = 76$ paired soma/axon recordings; see also refs 10, 11). In addition, involvement of an A-current is not consistent with the time course of the enhancement effect we observed (Fig. 1f), nor with the rightward shift in the distribution of evoked EPSP amplitudes (Fig. 2b, c). Similarly, we did not find a significant effect of hyperpolarizing current pulses (100 ms, 15–20 mV) ending 10 ms before the onset of the 5-ms depolarizing current pulse that initiated action potentials in the presynaptic neuron ($n = 6$ pairs).

We next examined the possibility that naturally occurring barrages of synaptic potentials might have a significant effect on the membrane potential of distal axons. By reducing the bath concentration of Ca^{2+} and Mg^{2+} to 1 mM each, we were able to induce a slow oscillation of network activity known as Up and Down states[12–15] ($n = 6$; Fig. 4a). This slow oscillation is associated with periods of recurrent excitatory and inhibitory activity within cortical networks, interspersed with periods of relative quiescence, and occurs naturally during periods of slow-wave sleep[16]. *In vivo*, these Up and Down states range between 10 and 20 mV in amplitude[15–17], but in our submerged cortical slices they were of more modest magnitude (9.2 ± 3.2 mV, $n = 20$ cells), presumably owing to the extensive loss of intracortical connectivity.

Performing simultaneous axonal and somatic whole-cell recordings from layer 5 cortical pyramidal cells ($n = 18$) revealed that the voltage fluctuations associated with synaptic barrages propagated long distances (>0.4 mm) along the main axon (Fig. 4e). The axonal form of synaptic barrages was a close copy of that recorded in the soma, with some attenuation at higher frequencies in the axon (Fig. 4b, $n = 18$). The axonal:somatic ratio of the integrated amplitude (mV × ms) of Up state synaptic activity decreased with distance from the soma, and this decrease could be well fitted ($r^2 = 0.82$, $P < 0.01$) with an exponential function with a length constant (λ) of 417 μm (Fig. 4e, $n = 18$), which is similar to the axonal length constant associated with constant depolarization of the soma (455 μm, $n = 28$). Our computational simulations indicate that even cortical neurons with extensive axonal arbors may also have axonal length constants in the hundreds of micrometres for low frequencies (see Supplementary Fig. 4), indicating that these long length constants are not an artefact of axotomy during slicing.

To further examine the electrophysiological communication of activity from the soma to the axon, we used the dynamic clamp technique[14,18] to inject Up-like conductance states (as well as broadband conductance noise) into the soma, and recorded the subsequent transfer of this activity down the axon (see Supplementary Figs 5 and 6; $n = 23$). These recordings revealed the rapid propagation of somatic membrane potential down the axon, again with attenuation at higher frequencies, with a decline in the overall amplitude time

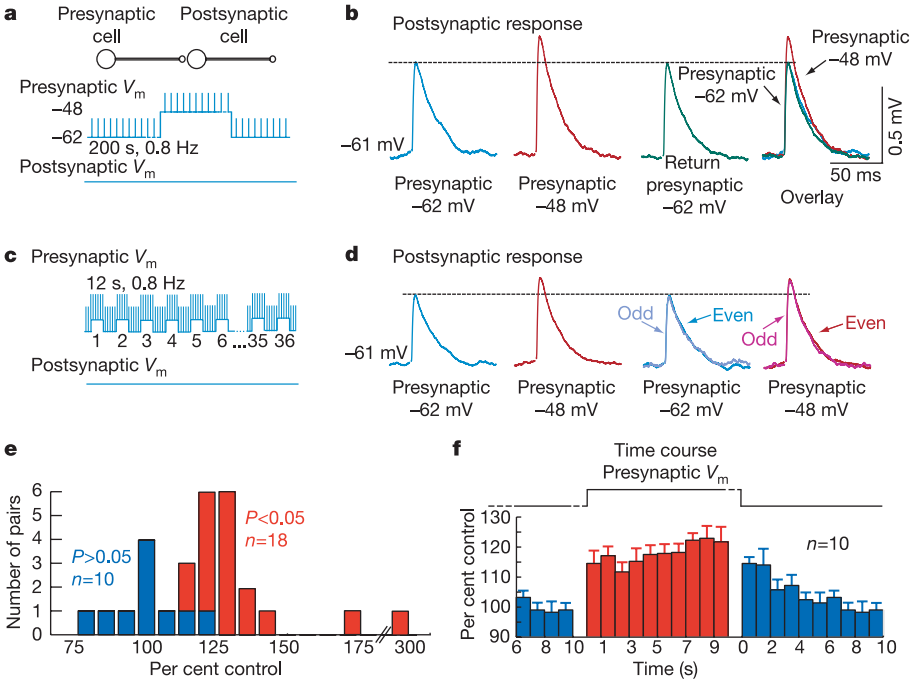


Figure 1 | Somatic depolarization results in an increase in the amplitude of evoked EPSPs in nearby neurons. **a**, A presynaptic layer 5 neuron was depolarized from rest (−62 mV in this cell) to near firing threshold (−48 mV in this cell), while being caused to spike at a rate of 0.8 Hz by the injection of 1-ms depolarizing current pulses. The resting and depolarized periods were 100–200 s each. **b**, Average EPSP amplitude at the two presynaptic somatic membrane potentials. See Supplementary Fig. 1 for morphology. **c**, The facilitating effect was also examined by intermixing 10–20-s periods of depolarization and hyperpolarization (typically 10–15 mV difference) of the soma of the presynaptic cell. **d**, Depolarization again resulted in a significant increase in the amplitude of the average evoked EPSP. Comparing the average EPSPs evoked on odd and even blocks within each depolarized or hyperpolarized state does not reveal any within-state difference, illustrating the stability of this effect. **e**, The median facilitated amplitude was 129% of the control, ranged from 112 to 294% and was seen in 18/28 pairs. **f**, Average time course of the facilitation and disfacilitation of EPSPs in cells that underwent the protocol in **c** and showed significant enhancement (1-s bin widths are shown with s.e.m.; see Supplementary Fig. 2).

© 2006 Nature Publishing Group

course of synaptic-like barrages that could be well fitted by an exponential function ($\lambda = 455\,\mu m$). Calculating the frequency-dependent transfer ratio from somatic conductance to axonal membrane potential revealed a strong transfer of moderate to low (<20 Hz) frequencies, and decreasing transfer with progressively higher frequencies (Supplementary Fig. 6; $n = 23$).

Layer 5 pyramidal neurons, like other cortical neurons, give rise to a local high density of axonal connections to other pyramidal and non-pyramidal cells[19–23] (Supplementary Figs 1, 4 and 7). Indeed, examination of the main axon and local axon collaterals of biocytin-filled layer 5 pyramidal cells from our slices revealed, on average, 155 (±79; $n = 14$ cells) putative synaptic boutons within 0.5-mm of the cell body, and 269 (±152) putative synaptic boutons within the first 1 mm (Fig. 4c and Supplementary Fig. 7). These values are probably a significant underestimate of local synaptic connectivity, owing to the cutting of axons and limitations of axonal staining using the slice technique (see Supplementary Figs 1 and 4).

Traditionally, somatic-to-axonal synaptic terminal communication in the mammalian brain is thought to occur solely through the rate and timing of action potentials. Here we demonstrate a new and important role for presynaptic somatic membrane potential in synaptic communication between nearby cortical neurons. The long length constant of layer 5 pyramidal cell axons allows for the rapid dissemination of changes in membrane potential to substantial numbers of nearby synaptic terminals, as well as influencing the duration of axonal action potentials. We hypothesize that one or both of these alterations underlies the depolarization-induced enhancement of synaptic transmission observed here[3,24,25].

We propose that the ability of the presynaptic somatic membrane potential to affect the magnitude of synaptic potentials is not limited to cortical layer 5 pyramidal cells, but may occur at many brain cell types that have presynaptic terminals that are electrotonically close to the cell body. This is especially relevant for the neocortex, where many different types of excitatory and inhibitory neurons form dense local synaptic networks[19–23]. The ability of the presynaptic dendrosomatic membrane potential to significantly influence synaptic transmission indicates that cells function in a more 'holistic' manner than previously appreciated, and has important functional consequences. For example, cortical neuronal networks that enter periods of persistent activity through recurrent excitation/inhibition[13]—which might underlie working memory, premotor planning and decision making—may do so in part through a conjoint increase in synaptic amplitudes owing to depolarization of the network. In addition, the large membrane potential changes that occur in central neurons in response to state changes (for example, waking versus slow-wave sleep)[16], the release of neuromodulatory neurotransmitters[26], sensory stimulation[27,28], epileptic seizures (see Supplementary Fig. 8) or spreading depression (a leading model for the aura of migraine headaches[29]) may strongly and directly influence synaptic transmission between affected neurons. On the basis of our findings, we suggest that local interneuronal communication in the brain is a

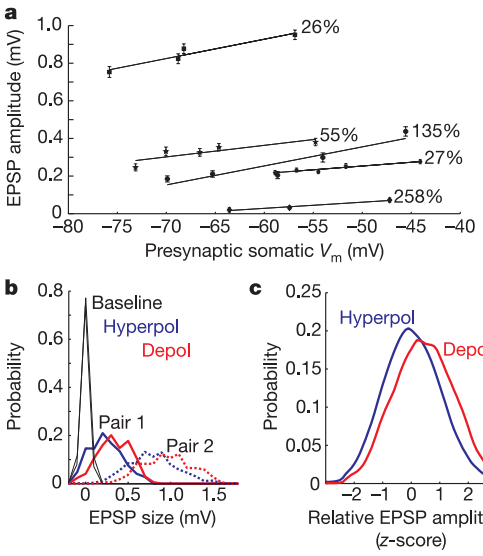


Figure 2 | Properties of EPSP enhancement. **a**, Plotting the average amplitude of the evoked EPSP versus the somatic membrane potential of the presynaptic neuron reveals continuous functions that are well fitted with a linear function ($n = 5$ pairs). To the right of each trace is the per cent enhancement of the EPSP recorded at the most depolarized, versus the most hyperpolarized, membrane potentials tested. Points show mean ± s.e.m. **b**, Two examples of histogram EPSP amplitude distributions at hyperpolarized and depolarized membrane potentials (following the protocol in Fig. 1a; both pairs show a significant shift, $P < 0.01$). The black line illustrates the level of baseline activity, using our measure of synaptic amplitude (see Methods). **c**, Depolarization significantly ($P < 0.01$) shifts the normalized EPSP amplitude histogram ($n = 15$ pairs) to the right. Normalization was performed by fitting the hyperpolarized amplitude distribution of each cell with a gaussian curve and then plotting the data such that the mean of the hyperpolarized state was 0 and the standard deviation was 1.

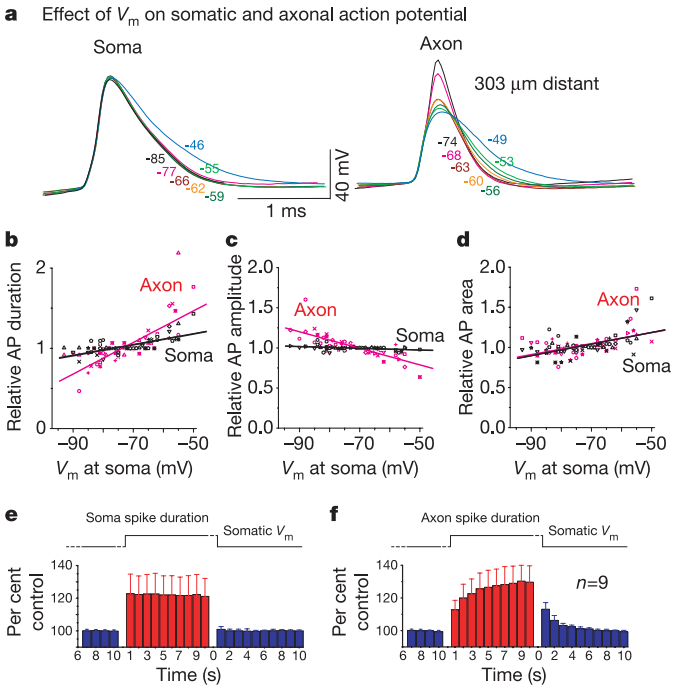


Figure 3 | Changes in somatic membrane potential affect the amplitude and duration of somatic and axonal action potentials. **a**, Simultaneous somatic and axonal (303 μm from soma) recording while the soma is depolarized or hyperpolarized to different levels by the injection of current. Action potentials are initiated with brief (5 ms) depolarizing current pulses through the somatic recording electrode. Raw, un-normalized traces are shown after at least 10 s with the baseline membrane potential at the value indicated. **b**, Plot of the duration of somatic (black) and axonal (red) action potentials, normalized to the duration recorded near −70 mV (soma 0.60 ± 0.11 ms, axon 0.55 ± 0.24 ms; measured at half height), versus the voltage at the soma for ten cells. **c**, Plot of the amplitude of somatic and axonal action potentials after normalization to the value obtained at a membrane potential of −70 mV (soma 91.2 ± 6.3 mV; axon 71.0 ± 14.4 mV) versus somatic membrane potential. **d**, Plot of the action potential area (mV × ms) versus somatic membrane potential after normalization to the value obtained at −70 mV (soma 26.3 ± 3.2 mV ms^{-1}; axon 16.4 ± 3.9 mV ms^{-1}). **e**, **f**, Time course of changes in the duration of action potentials in the soma (**e**) and axon (**f**; average distance of 215 μm) during the indicated changes in membrane potential (see Supplementary Fig. 2). The average spike duration corresponding to 100% was 0.61 ms for soma, 0.54 ms for axon.

© 2006 Nature Publishing Group

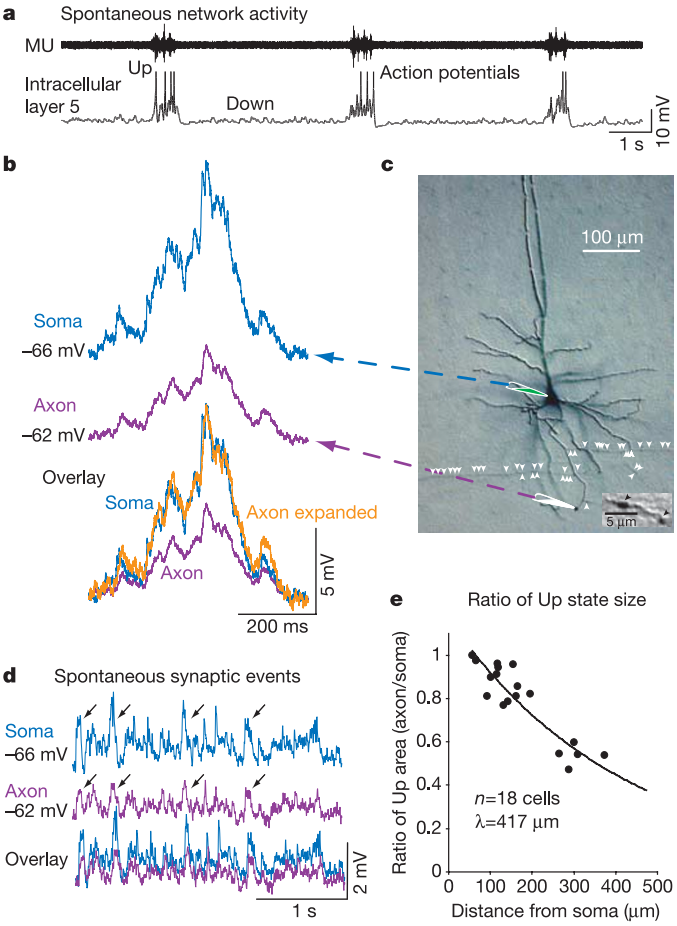


Figure 4 | Spontaneous barrages of synaptic activity propagate down the axon. **a**, Simultaneous extracellular multiple unit (MU) and somatic whole-cell recording in layer 5 during the generation of recurrent network activity of the Up state, interspersed with relatively quiet periods of the Down state. **b**, Simultaneous recording of an Up state in the soma and cut end of the main axon (266 µm from the soma). The bottom traces are an overlay of axonal (purple) and somatic (blue) recordings of synaptic activity, along with a version of the axonal recording that has been expanded to match the peak amplitude of the somatic recording (orange). **c**, Morphology of the recorded cell. White arrowheads indicate putative presynaptic boutons along the axon collaterals in this focal plane. Inset shows an example of two putative *en passant* boutons. Note the large number of boutons that seem to be electronically close to the soma. **d**, Even during quiescent periods, spontaneous synaptic events (arrows point to examples) are recorded in both the soma and the cut end of the main axon of the cell in **c**. **e**, Comparison of the amplitude (area) of Up states at the soma and the cut end of the axon in different layer 5 neurons reveals an orderly decrease in the amplitude of spontaneous synaptic activity with distance from the soma. The calculated length constant of the axon is 417 µm.

result of discrete, action-potential-dependent triggered release that is graded by presynaptic membrane potential.

Note added in proof: A recent study has demonstrated a similar phenomenon to that described here at the synaptic connection between granule cells and CA3 pyramidal cells in the hippocampus[31]. Together, these findings reveal the mixed triggered and graded (analogue) nature of synaptic transmission in the mammalian brain, even over relatively long distances.

METHODS

See Supplementary Information for full descriptions of the methods used. Experiments were performed using standard slice and patch-clamp procedures. Briefly, 0.3-mm thick slices of ferret cortex (7–10-weeks old), typically from the prefrontal region but also from the somatosensory area, were incubated at 35 °C and then maintained *in vitro* in a submerged-style recording chamber at 36.5 °C on an upright infrared-differential interference contrast (IR-DIC) microscope equipped with fluorescence for the visualization of axonal profiles. The artificial cerebrospinal fluid (ACSF) contained 126 mM NaCl, 2.5 mM KCl, 2 mM $MgSO_4$, 2 mM $CaCl_2$, 26 mM $NaHCO_3$, 1.25 mM NaH_2PO_4, 25 mM dextrose (315 mOsm, pH 7.4). For only those recordings in which the slow oscillation was examined in the submerged chamber, the ACSF solution was modified to contain 1 mM $MgSO_4$, 1 mM $CaCl_2$ and 3.5 mM KCl[12–14]. The membrane potentials in our whole-cell recordings were not corrected for Donnan liquid junction potentials, which typically range between 5 and 15 mV (ref. 30).

Whole-cell recordings were achieved from both soma and the cut end of the main axon using a Multiclamp 700B or Axoclamp 2B amplifier (Axon Instruments). Patch pipettes (somatic 5–6 MΩ, axonal 9–15 MΩ) were filled with 140 mM potassium gluconate, 3 mM KCl, 2 mM $MgCl_2$, 2 mM Na_2ATP, 10 mM HEPES, 0.025 mM BAPTA, Alexa Fluo 488 (100 µM; for axonal recording experiments only), 0.2% biocytin, pH 7.2 with KOH (288 mOsm). Activation of nearby (within 60 µm) morphologically identified pyramidal cells resulted in EPSPs that (1) were blocked by bath application of the non-NMDA glutamatergic receptor antagonist CNQX (10 µM in bath; $n = 4$), (2) decayed with an exponential time course, and (3) were not followed by inhibitory synaptic potentials (Fig. 1b). Data were analysed only if the evoked EPSP did not exhibit significant run-down or other instability, as shown by a statistically significant change in the amplitude of the EPSP either between the two control periods (when the presynaptic membrane potential was at rest before and after the depolarizing period) or between the first and last third of the interspersed control periods (as in the protocol of Fig. 1c).

For simultaneous somatic and axonal whole-cell recordings, the terminal 'bleb' of the axon on the surface of the slice was identified through brief (less than 20 s) exposure of the cell to fluorescence. Recordings with access resistance (monitored frequently) higher than 25 MΩ for somatic recording or 45 MΩ for axonal recording were discarded. Bridge balance and capacitance neutralization were carefully adjusted before and after every experimental protocol. After a recording was completed, the slice was transferred to 4% paraformaldehyde in 0.1 M phosphate buffer for subsequent immunostaining and visualization.

EPSP magnitudes were measured by first carefully identifying presynaptic action potential time courses. The average EPSP in the postsynaptic cell was calculated synchronized to the timing of presynaptic action potentials, and the timing of the peak of the average EPSP was determined. The amplitude of each evoked EPSP on single trials was taken as the difference between the postsynaptic membrane potential at the peak time of the average EPSP after the action potential and the membrane potential before onset of the current pulse evoking the action potential. Baseline activity was measured as the difference in membrane potential over the same time delay, but without activation of a presynaptic spike. Unless otherwise stated, statistical tests were performed using Student's *t*-tests. Values are presented as mean ± s.d. in the text and mean ± s.e.m. in the figures.

Received 30 December 2005; accepted 16 March 2006.
Published online 12 April 2006.

1. Stuart, G., Schiller, J. & Sakmann, B. Action potential initiation and propagation in rat neocortical pyramidal neurons. *J. Physiol. (Lond.)* **505,** 617–632 (1997).
2. Mainen, Z. F., Joerges, J., Huguenard, J. R. & Sejnowski, T. J. A model of spike initiation in neocortical pyramidal neurons. *Neuron* **15,** 1427–1439 (1995).
3. Awatramani, G. B., Price, G. D. & Trussell, L. O. Modulation of transmitter release by presynaptic resting potential and background calcium levels. *Neuron* **48,** 109–121 (2005).
4. Nicholls, J. & Wallace, B. G. Quantal analysis of transmitter release at an inhibitory synapse in the central nervous system of the leech. *J. Physiol. (Lond.)* **281,** 171–185 (1978).
5. Shimahara, T. & Tauc, L. Multiple interneuronal afferents to the giant cells in Aplysia. *J. Physiol. (Lond.)* **247,** 299–319 (1975).
6. Shapiro, E., Castellucci, V. F. & Kandel, E. R. Presynaptic membrane potential affects transmitter release in an identified neuron in *Aplysia* by modulating the Ca^{2+} and K^+ currents. *Proc. Natl Acad. Sci. USA* **77,** 629–633 (1980).
7. Ivanov, A. I. & Calabrese, R. L. Modulation of spike-mediated synaptic transmission by presynaptic background Ca^{2+} in leech heart interneurons. *J. Neurosci.* **23,** 1206–1218 (2003).
8. Storm, J. F. Temporal integration by a slowly inactivating K^+ current in hippocampal neurons. *Nature* **336,** 379–381 (1988).
9. Debanne, D., Guerineau, N. C., Gahwiler, B. H. & Thompson, S. M. Action-potential propagation gated by an axonal I_A-like K^+ conductance in hippocampus. *Nature* **389,** 286–289 (1997).
10. Cox, C. L., Denk, W., Tank, D. W. & Svoboda, K. Action potentials reliably invade axonal arbors of rat neocortical neurons. *Proc. Natl Acad. Sci. USA* **97,** 9724–9728 (2000).

© 2006 Nature Publishing Group

11. Koester, H. J. & Sakmann, B. Calcium dynamics associated with action potentials in single nerve terminals of pyramidal cells in layer 2/3 of the young rat neocortex. *J. Physiol. (Lond.)* **529,** 625–646 (2000).
12. Sanchez-Vives, M. V. & McCormick, D. A. Cellular and network mechanisms of rhythmic recurrent activity in neocortex. *Nature Neurosci.* **3,** 1027–1034 (2000).
13. Shu, Y., Hasenstaub, A. & McCormick, D. A. Turning on and off recurrent balanced cortical activity. *Nature* **423,** 288–293 (2003).
14. Shu, Y., Hasenstaub, A., Badoual, M., Bal, T. & McCormick, D. A. Barrages of synaptic activity control the gain and sensitivity of cortical neurons. *J. Neurosci.* **23,** 10388–10401 (2003).
15. Hasenstaub, A. *et al.* Inhibitory postsynaptic potentials carry synchronized frequency information in active cortical networks. *Neuron* **47,** 423–435 (2005).
16. Steriade, M., Timofeev, I. & Grenier, F. Natural waking and sleep states: a view from inside neocortical neurons. *J. Neurophysiol.* **85,** 1969–1985 (2001).
17. Steriade, M., Nunez, A. & Amzica, F. A novel slow (<1 Hz) oscillation of neocortical neurons *in vivo*: depolarizing and hyperpolarizing components. *J. Neurosci.* **13,** 3252–3265 (1993).
18. Dorval, A. D., Christini, D. J. & White, J. A. Real-time linux dynamic clamp: a fast and flexible way to construct virtual ion channels in living cells. *Ann. Biomed. Eng.* **29,** 897–907 (2001).
19. Binzegger, T., Douglas, R. J. & Martin, K. A. Axons in cat visual cortex are topologically self-similar. *Cereb. Cortex* **15,** 152–165 (2005).
20. Binzegger, T., Douglas, R. J. & Martin, K. A. A quantitative map of the circuit of cat primary visual cortex. *J. Neurosci.* **24,** 8441–8453 (2004).
21. Gilbert, C. D. & Wiesel, T. N. Clustered intrinsic connections in cat visual cortex. *J. Neurosci.* **3,** 1116–1133 (1983).
22. Markram, H., Lubke, J., Frotscher, M., Roth, A. & Sakmann, B. Physiology and anatomy of synaptic connections between thick tufted pyramidal neurones in the developing rat neocortex. *J. Physiol. (Lond.)* **500,** 409–440 (1997).
23. Peters, A. & Jones, E. G. (eds) *Cerebral Cortex* **Vol. 1** (Plenum Press, New York, 1984).
24. Jackson, M. B., Konnerth, A. & Augustine, G. J. Action potential broadening and frequency-dependent facilitation of calcium signals in pituitary nerve terminals. *Proc. Natl Acad. Sci. USA* **88,** 380–384 (1991).
25. Geiger, J. R. & Jonas, P. Dynamic control of presynaptic Ca^{2+} inflow by fast-inactivating K^+ channels in hippocampal mossy fiber boutons. *Neuron* **28,** 927–939 (2000).
26. McCormick, D. A. Neurotransmitter actions in the thalamus and cerebral cortex and their role in neuromodulation of thalamocortical activity. *Prog. Neurobiol.* **39,** 337–388 (1992).
27. Carandini, M. & Ferster, D. A tonic hyperpolarization underlying contrast adaptation in cat visual cortex. *Science* **276,** 949–952 (1997).
28. Sanchez-Vives, M. V., Nowak, L. G. & McCormick, D. A. Membrane mechanisms underlying contrast adaptation in cat area 17 *in vivo*. *J. Neurosci.* **20,** 4267–4285 (2000).
29. Welch, K. M. Contemporary concepts of migraine pathogenesis. *Neurology* **61,** S2–S8 (2003).
30. Fricker, D., Verheugen, J. A. & Miles, R. Cell-attached measurements of the firing threshold of rat hippocampal neurones. *J. Physiol. (Lond.)* **517,** 791–804 (1999).
31. Alle, H. & Geiger, J. R. P. Combined analog and action potential coding in hippocampal mossy fibers. *Science* **311,** 1290–1293 (2006).

Supplementary Information is linked to the online version of the paper at www.nature.com/nature.

Acknowledgements This work was supported by the NIH (D.A.M.), the Howard Hughes Foundation (A.H.) and the Kavli Institute for Neuroscience.

Author Contributions Y.S. performed all recordings, A.H. analysed the data, A.D. did cell reconstructions, Y.Y. performed computational models, and D.A.M. wrote the paper and helped design experiments. All authors discussed the results and commented on the manuscript.

Author Information Reprints and permissions information is available at npg.nature.com/reprintsandpermissions. The authors declare no competing financial interests. Correspondence and requests for materials should be addressed to D.A.M. (david.mccormick@yale.edu).

© 2006 Nature Publishing Group